Radiative Lifetimes of The Perturbed 6snf $^3F_3$, $^1F_3$, and $^3F_4$ Rydberg Sequences of Barium

M. A. Zaki Ewiss

Physics Department, Faculty of Science, Cairo University, Giza, Egypt

Z. Naturforsch. **52a**, 702–708 (1997); received April 1, 1997

Extensive new results for the natural radiative lifetimes of the perturbed odd-parity 6snf $^3F_3$, $^1F_3$, and $^3F_4$ sequences of barium (with $11 \leq n \leq 40$, $11 \leq n \leq 40$ and $13 \leq n \leq 40$, respectively) have been calculated. The calculations were performed in the framework of multichannel quantum defect theory. The contributions to the transition probabilities of all known even-parity levels of the 6snd and 6sng configurations together with their perturber states and connected via the electric dipole operator with the 6snf $^3F_3$, $^1F_3$, and $^3F_4$ levels, are considered.

The results for the 6snf $^1F_3$ and $^3F_4$ sequences, in contrast with those for the 6snf $^3F_3$ series, show strong deviation from a hydrogenic scaling law. This deviation reflects the extended perturbations of these levels by some of the doubly excited states of the same parity.

1. Introduction

Highly excited and autoionizing states of atoms have been the subject of extensive studies in several laboratories. In particular, the alkaline-earth elements (Mg, Ca, Sr and Ba) have been studied using different spectroscopic techniques [1–21]. It is known that these atoms have considerably more complicated spectra when compared with the spectra of the alkali atoms, because of the addition of a second electron outside the closed shells. The two electrons can couple to many different configurations and interactions between close-lying configurations are frequent. Such interactions are reflected in the primary energy level structure, but also in more subtle appearances like Zeeman and Stark effects, fine and hyperfine structure and Lande'-factors. The perturbations also affect the radiative properties of the atomic levels.

The odd-parity Rydberg seris of barium have been subject of several detailed spectroscopic studies. The 6snp levels were first studied by Garton and Tomkins [8] in a classical absorption experiment. In addition to level energies of the Rydberg P-states up to $n = 75$, valuable information regarding the autoionizing states with orbital angular momentum $l = 1$ was obtained. Armstrong et al. [9], expanded this study of the bound $l = 1$ states to levels with $^3P_1$ and $^3P_2$ character, applying a three-step excitation scheme with pulsed tunable dye lasers. They also performed a multichannel quantum defect theory (MQDT) analysis of their results. The 6snp $^1P_1$ series was found to be more strongly perturbed than the 6snp $^3P_1$ series. The perturber states belong to 5dnp and 5dnf configurations. The level energies of these autoionizing configurations were determined by Abu-Taleb [10], using a two step laser excitation process.

Accurate energy values of the 6snf $^1F_3$ and $^3F_{2,3,4}$ levels with $10 \leq n \leq 50$ were measured by Post et al. [11, 12], using high resolution CW laser spectroscopic techniques. In addition to strong singlet-triplet mixing between $^1F_3$ and $^3F_3$ levels it was found that these levels are strongly perturbed by the $J = 3$ levels of the 5d8p configuration. Also the $^3F_2$ and $^3F_4$ levels are perturbed by the $J = 2$ and $J = 4$ levels of the 5d8p and 5d4f configurations. Zaki Ewiss et al. [13–15] measured the Stark effect of these Rydberg series, using CW UV-laser excitation from metastable 6s5d states. In these measurements the series perturbations could be verified.

Although, the availability of tunable dye laser systems facilitated measurements of natural radiative lifetimes of atomic levels through selective state excitation, information on radiative lifetimes of the 6snf $^1F_3$ and $^3F_{2,3,4}$ ($n \geq 11$) levels of Ba I is scarce. Unfortunately, the detection of the exponential decay of these highly excited levels suffers from deleterious black body radiation effects. Values for these lifetimes are important, not only to investigate perturbations of atomic levels, but also for the interpretation of data in the fields of plasma- and astro-physics.

Reprint requests to Dr. M. A. Zaki Ewiss;
Fax: 202-572 75 56, E-mail: MZEWISS@FRCU.EUN.EG.

0932-0784 / 97 / 1000-0702 $ 06.00 © – Verlag der Zeitschrift für Naturforschung, D-72027 Tübingen

In this paper, extensive theoretical results for the natural radiative lifetime of the perturbed odd-parity 6snf $^3F_3$, $^1F_3$, and $^3F_4$ sequences of barium (with $11 \leq n \leq 40$, $11 \leq n \leq 40$ and $13 \leq n \leq 40$, respectively) will be presented. The calculation is based on the multichannel quantum defect theory (MQDT) analysis. A large number of experimental energy values for these series as well as those series contributing to the transition probabilities are used to generate wave functions.

2. Theoretical Background

The natural radiative lifetime $\tau(\gamma J)$ of an excited atomic level $|\gamma J\rangle$ is defined in terms of intrinsic atomic properties (J is the total angular momentum quantum number and γ denotes the other quantum numbers describing the atomic states). The level $|\gamma J\rangle$ with energy $W_{\gamma J}$ and degeneracy $g_i = (2J + 1)$ can decay to the level $|\gamma' J'\rangle$ with energy $W_{\gamma' J'}$ under emission of a photon with frequency determined by

$$h\nu = W_{\gamma J} - W_{\gamma' J'} . \tag{1}$$

This process is described with the electric dipole operator **P**. Commonly, many decay channels $\gamma J \rightarrow \gamma' J'$ are available; with each channel a transition probability is connected:

$$\cdot A(\gamma' J', \gamma J) \approx |\langle \gamma' J' | \bar{P} | \gamma J \rangle|^2 . \tag{2}$$

The total transition probability is

$$A(\gamma J) = \sum_{\gamma' J'} A(\gamma' J', \gamma J) . \tag{3}$$

The lifetime is defined as

$$\tau(\gamma J) = \frac{1}{A(\gamma J)} . \tag{4}$$

The summation extends over all electronic states $|\gamma' J'\rangle$ with parity opposite to the parity of the $|\gamma J\rangle$ state, satisfying the well known the $|\Delta J| = \pm 1, 0$ selection rules for dipole transitions.

The matrix element of the electronic dipole operator can be expressed in terms of the reduced matrix element $R^{\gamma J}_{\gamma' J'}$ using standard angular momentum algebra. The resulting transition probability is expressed as [16]

$$A(\gamma' J', \gamma J) = \frac{64\pi^4 (W_{\gamma J} - W_{\gamma' J'}) |R^{\gamma J}_{\gamma' J'}|^2}{3 h^4 c^3 (2J + 1)} . \tag{5}$$

The quantity $|R^{\gamma J}_{\gamma' J'}|^2$ is called the line strength (S).

The calculation of the transition probability requires the evaluation of the reduced matrix elements $R^{\gamma J}_{\gamma' J'}$ of the electric dipole operator. This evaluation requires knowledge of the wave functions of the states involved. Once the wave functions, specified in the basis of MQDT channels are known the dipole matrix element can be reduced further to single-electron radial integrals of the type

$$R^{\gamma J}_{\gamma' J'} = \int_0^\infty R_{n1}(r)\, r\, R_{n' 1'}(r)\, \mathrm{d}r . \tag{6}$$

Here $R_{nl}(r)$ is the radial part of the wave function of the nl-electron. This integral can be calculated in Coulomb approximation assuming generalized hydrogenic radial functions for the highly excited states normalized to the experimental level energies [17]. The feasibility of the procedure outlined here was tested by the calculation of the radiative lifetime of 6snd $^{1,3}D_2$ Rydberg levels of barium ($17 \leq n \leq 35$) by Aymar and Camus [18] and on the polarizabilities of barium 6snf $^1F_3$, $^3F_{2,3,4}$ Rydberg levels [13–15].

3. Results

3.1 General

The calculation of the natural radiative lifetime of the 6snf $^3F_3$, $^1F_3$, and $^3F_4$ Rydberg sequences requires knowledge of the level energies and wave functions of these odd-parity $J = 3$ and 4 series as well as of the contributing even-parity levels of the 6snd and 6sng configurations, together with their perturber states in the energy region 41 100 cm^{-1}–41 970 cm^{-1}.

Accurate level energies (0.01 cm^{-1}) of the 6snf $^3F_3$, $^1F_3$, and $^3F_4$ Rydberg series in the interval $n = 10–50$ and an MQDT analysis of these $J = 3$ and $J = 4$ levels were reported by Post et al. [11]. The 6snf $^1F_3$ Rydberg series is perturbed by the 5d8p $^3F_3$ and $^3D_3$ doubly-excited levels near $n = 16$ and by 5d8p $^1F_3$ near $n = 20$. It was found that the latter perturbation extends over a large number of Rydberg levels of the 6snf $^1F_3$ series. The 6snf $^3F_3$ series was found to be slightly affected by the presence of the 5d8p levels. In Fig. 1 a Lu-Fano plot for the 6snf $J = 3$ levels is reproduced from [11]. The accurate measurements of the hyperfine structure and isotope shifts in the 6snf Rydberg series by Post et al. [12], combined with the MQDT analysis of $J = 3$ level energies, provide reliable information on the wave functions of the 6snf $^{1,3}F_3$ series in terms of singlet-triplet mixing coefficients and admixtures of perturber character for most n-values.

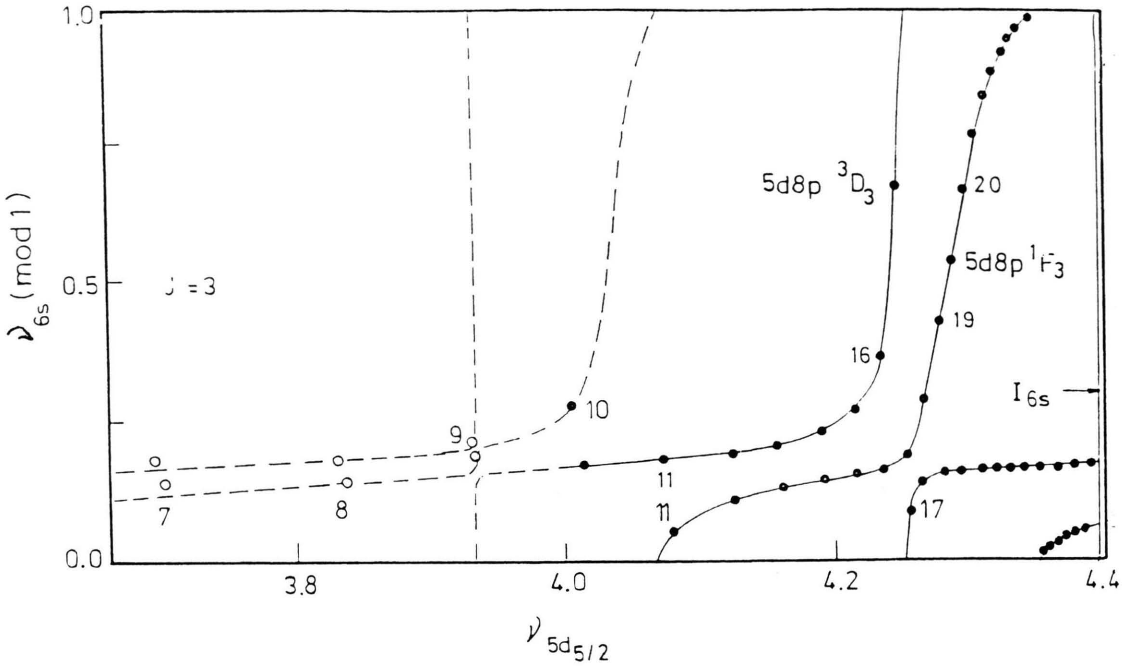

Fig. 1. Lu-Fano plot of the 6snf $J = 3$ levels of Ba I, reproduced from [11].

Also, a two-channel MQDT model has been developed to fit the accurate level energies of the 6snf $^3F_4$ series and the 5dnp $^3F_4$ ($n = 7, 8$) perturbing levels [11]. The MQDT wave functions for these levels were tested subsequently in the hyperfine structure and isotope shift data of Post et al. [12] and the quadratic Stark effect measurements of Zaki Ewiss et al. [15], resulting in good agreement with observations. In [12], it was found that the 5d7p $^3F_4$ level is located close to the 6s5f $^3F_4$ level, while the 5d8p $^3F_4$ level lies in between 6s18f and 6s19f $^3F_4$. The interaction with the 5d8p $^3F_4$ level affects many Rydberg levels, notably in the region $n = 15-25$. Due to this perturbation the quantum defect of the 6s20f $^3F_4$ level is nearly zero, resulting in a near degeneracy with levels with higher orbital angular momentum L. This made it difficult to measure the quadratic Stark effect in this level [15]. In this case, the excitation of the 6s20f $^3F_4$ level in the presence of an electric field quickly results in the evolution of a linear Stark-manifold. In Fig. 2 the Lu-Fano plot of the 6snf $^3F_4$ series is reproduced [11].

Extensive MQDT analyses are available for the level energies of the even-parity 6snd and 6sng configurations as well. The levels of the 6snd configuration are perturbed by doubly-excited 5d7s, 5d8s and 5d6d

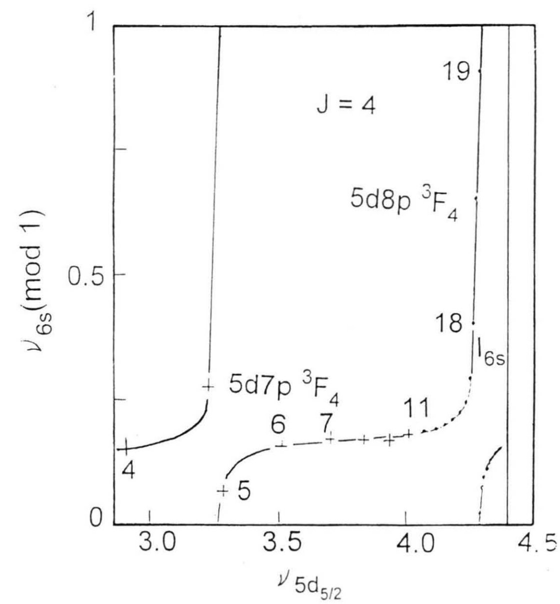

Fig. 2. Lu-Fano plot of the 6snf $J = 4$ levels of Ba I, reproduced from [11].

configurations for $n \leq 10$ and by 5d7d levels for $n > 10$ [16, 18–20]. Including hyperfine structure and Lande'-factor measurements Aymar [20], performed a nine-channel MQDT analysis for the 6snd $^{1,3}D_2$ levels. In addition to strong singlet-tripling mixing in the series, she perfound that the $^1D_2$ levels are perturbed near $n = 12$, 14 and 26. Camus et al. [19] have measured energies for the 6snd $^3D_3$ levels. The levels are perturbed near $n = 10, 12, 17, 21$ and 27 by 5d7d $J = 3$ perturber states. These perturbers also affect the 6sng $^3G_3$ Rydberg series [13, 21].

A wealth of information on the even-parity 6sng $^{1,3}G_4$ and $^3G_5$ levels, including experimental energy values, hyperfine structure data and MQDT wave functions of these levels together with their perturber states, has been collected by Vassen et al. [21, 22].

Wave functions based on MQDT channels for the 6snf $^3F_3$, $^1F_3$, and $^3F_4$ Rydberg levels as well as for the contributing levels of the 6snd and 6sng configurations together with their perturber states have been used in the evaluation of the reduced matrix element $R^{\gamma J}_{\gamma' J'}$. Integral (6), was calculated in Coulomb approximation using the numerical method of Zimmerman et al. [23], assuming generalized hydrogenic radial functions for the highly excited states, normalized to the experimental level energies.

3.2 Natural Radiative Lifetimes in the 6snf $^3F_3$ Sequence

The values of the natural radiative lifetime of the 6snf $^3F_3$ sequence of Ba I are calculated from (3) and (4). The results are given in Table 1. Figure 3, shows the ln-ln plot of the values of the lifetime versus the effective principal quantum number n^*. The linear fit with slope 3 satisfies a hydrogenic scaling model ($\tau \propto n^{*3}$). In Table 2, the branching ratios corresponding to transitions of 6snf $^3F_3$ levels to all lower even-parity 6snd $^{1,3}D_2$, $^3D_3$ and 6sng $^{1,3}G_4$ and $^3G_3$ levels are presented. It should be noted that the contributions of the decay to 6snd $^{1,3}D_2$ and 6sng $^{1,3}G_4$ levels dominate over the contributions of the decay to 6snd $^3D_3$ and 6sng $^3G_3$ levels.

3.3 Natural Radiative Lifetimes in the 6snf $^1F_3$ Sequence

In Table 3, calculated values for the radiative lifetimes (τ) of the 6snf $^1F_3$ ($11 \leq n \leq 40$) levels of Ba I are given. In Fig. 4, the ln-ln plot of τ versus n^* is shown.

Table 1. Theoretical values for radiative lifetime of the 6snf $^3F_3$ sequence of Ba I.

Level	τ (μs)	Level	τ (μs)
6s11f $^3F_3$	11.6	6s25f $^3F_3$	156.0
6s12f $^3F_3$	17.7	6s26f $^3F_3$	174.0
6s13f $^3F_3$	19.7	6s27f $^3F_3$	189.0
6s14f $^3F_3$	25.9	6s28f $^3F_3$	211.0
6s15f $^3F_3$	36.5	6s29f $^3F_3$	240.0
6s16f $^3F_3$	42.6	6s30f $^3F_3$	266.0
6s17f $^3F_3$	52.9	6s31f $^3F_3$	294.0
6s18f $^3F_3$	49.8	6s32f $^3F_3$	325.0
6s19f $^3F_3$	60.2	6s33f $^3F_3$	351.0
6s20f $^3F_3$	71.9	6s34f $^3F_3$	388.0
6s21f $^3F_3$	90.7	6s35f $^3F_3$	423.0
6s22f $^3F_3$	101.7	6s36f $^3F_3$	477.0
6s23f $^3F_3$	113.0	6s38f $^3F_3$	547.0
6s24f $^3F_3$	132.0	6s40f $^3F_3$	631.0

Table 2. Branching ratios $a(^{1,3}D_2)^a$, $a(^3D_3)^b$, $a(^3G_3)^c$, and $a(^{1,3}G_4)^d$ for the 6snf $^3F_3$ levels of Ba I.

n	$a(^{1,3}D_2)$	$a(^3D_3)$	$a(^3G_3)$	$a(^{1,3}G_4)$
11	0.278	0.060	0.010	0.651
12	0.463	0.113	0.015	0.409
13	0.585	0.121	0.010	0.284
14	0.588	0.043	0.012	0.357
15	0.521	0.042	0.015	0.422
16	0.494	0.035	0.015	0.456
17	0.402	0.045	0.002	0.551
18	0.678	0.060	0.014	0.248
19	0.637	0.053	0.025	0.285
20	0.619	0.053	0.018	0.310
21	0.600	0.051	0.028	0.321
22	0.588	0.050	0.025	0.333
23	0.583	0.048	0.025	0.340
24	0.576	0.051	0.030	0.343
25	0.495	0.029	0.040	0.436
26	0.550	0.049	0.034	0.367
27	0.549	0.047	0.033	0.371
28	0.540	0.046	0.034	0.380
29	0.526	0.046	0.035	0.393
30	0.518	0.045	0.036	0.401
31	0.510	0.044	0.036	0.410
32	0.504	0.043	0.037	0.416
33	0.503	0.041	0.037	0.419
34	0.494	0.040	0.038	0.428
35	0.488	0.039	0.038	0.435
36	0.475	0.038	0.039	0.448
38	0.470	0.036	0.039	0.455
40	0.462	0.033	0.039	0.466

[a] $a(^{1,3}D_2)$ is the branching ratio corresponding to the transitions from the 6snf $^3F_3$ levels to the 6snd $^{1,3}D_2$ levels.
[b] $a(^3D_3)$ is the branching ratio corresponding to the transitions from the 6snf $^3F_3$ levels to the 6snd $^3D_2$ levels.
[c] $a(^3G_3)$ is the branching ratio corresponding to the transitions from the 6snf $^3F_3$ levels to the 6sng $^3G_3$ levels.
[d] $a(^{1,3}G_4)$ is the branching ratio corresponding to the transitions from the 6snf $^3F_3$ levels to the 6sng $^{1,3}G_4$ levels.

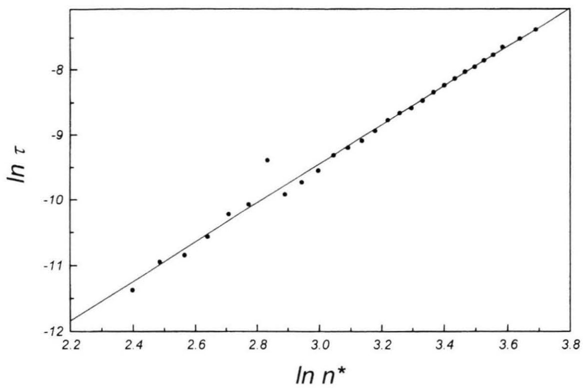

Fig. 3. ln−ln plot of the natural radiative lifetimes versus the effective principal quantum number of the odd-parity 6snf $^3F_3$ Rydberg series of Ba I.

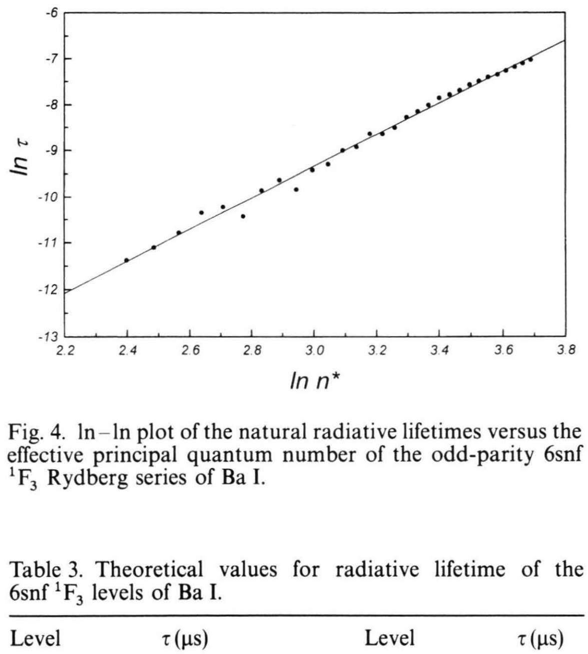

Fig. 4. ln−ln plot of the natural radiative lifetimes versus the effective principal quantum number of the odd-parity 6snf $^1F_3$ Rydberg series of Ba I.

Table 3. Theoretical values for radiative lifetime of the 6snf $^1F_3$ levels of Ba I.

Level	τ (μs)	Level	τ (μs)
6s11f $^1F_3$	11.5	6s25f $^1F_3$	177.0
6s12f $^1F_3$	15.1	6s26f $^1F_3$	203.0
6s13f $^1F_3$	20.8	6s27f $^1F_3$	265.0
6s14f $^1F_3$	32.1	6s28f $^1F_3$	291.0
6s15f $^1F_3$	36.5	6s29f $^1F_3$	235.5
6s16f $^1F_3$	29.7	6s30f $^1F_3$	391.0
6s17f $^1F_3$	84.0	6s31f $^1F_3$	418.9
6s18f $^1F_3$	65.8	6s32f $^1F_3$	458.1
6s19f $^1F_3$	54.0	6s33f $^1F_3$	517.7
6s20f $^1F_3$	81.3	6s34f $^1F_3$	560.2
6s21f $^1F_3$	91.8	6s35f $^1F_3$	609.5
6s22f $^1F_3$	123.2	6s36f $^1F_3$	643.0
6s23f $^1F_3$	133.3	6s38f $^1F_3$	760.9
6s24f $^1F_3$	177.5	6s40f $^1F_3$	892.5

The linear fit of these calculated values with slope 3.6 shows a strong deviation from the hydrogenic model. In Table 4, the branching ratios correspoding to transitions of the 6snf $^1F_3$ levels to all lower even-parity 6snd $^{1,3}D_2$, $^3D_3$ and 6sng $^{1,3}G_4$ and $^3G_3$ levels are given. At $n = 18$ the branching ratio $a(^{1,3}G_4)$ has the large value of 0.917, whereas a remarkable decrease of this value in the region $n = 21-24$ in comparison with the value of the branching ratio $a(^{1,3}D_2)$ is found. This effect relates to the strong perturbation of the 6snf $^1F_3$ levels near $n = 17$ and in between $n = 19$ and 20 as discussed above. The latter perturbation with the 5d8p $^1F_3$ level shifts the 6snf $^1F_3$ levels in the region $n = 20-24$ downward with respect to the level energies of the 6sng $^{1,3}G_4$ level. This results in a lower value for the branching ratio. Similar effects were observed in the calculation of the contributions of the 6sng $^{1,3}G_4$ levels to the polarizabilities of the 6snf $^1F_3$ series near $n = 17$ and at $n = 20-24$ [14].

Table 4. Branching ratios $a(^{1,3}D_2)^a$, $a(^3D_3)^b$, $a(^3G_3)^c$, and $a(^{1,3}G_4)^d$ for the 6snf $^1F_3$ levels of Ba I.

n	$a(^{1,3}D_2)$	$a(^3D_3)$	$a(^3G_3)$	$a(^{1,3}G_4)$
11	0.655	0.194	1.0×10^{-3}	0.150
12	0.624	0.120	7.0×10^{-3}	0.249
13	0.341	0.192	14.0×10^{-3}	0.453
14	0.341	0.022	18.0×10^{-3}	0.619
15	0.338	0.017	19.0×10^{-3}	0.626
16	0.606	0.011	18.0×10^{-3}	0.365
17	0.560	0.045	28.0×10^{-3}	0.367
18	0.070	0.011	1.0×10^{-3}	0.917
19	0.368	0.030	6.0×10^{-3}	0.596
20	0.683	0.053	0.8×10^{-3}	0.263
21	0.883	0.027	0.2×10^{-3}	0.090
22	0.889	0.057	0.3×10^{-3}	0.053
23	0.921	0.027	0.1×10^{-3}	0.052
24	0.858	0.049	0.9×10^{-3}	0.092
25	0.820	0.048	1.0×10^{-3}	0.131
26	0.674	0.036	1.0×10^{-3}	0.289
27	0.791	0.020	1.0×10^{-3}	0.188
28	0.685	0.035	9.0×10^{-3}	0.271
29	0.721	0.010	1.0×10^{-3}	0.268
30	0.681	1.5×10^{-2}	0.7×10^{-3}	0.303
31	0.512	0.7×10^{-2}	1.0×10^{-3}	0.480
32	0.641	0.9×10^{-2}	0.8×10^{-3}	0.348
33	0.607	0.9×10^{-2}	9.6×10^{-4}	0.383
34	0.591	0.89×10^{-2}	1.0×10^{-3}	0.399
35	0.563	0.85×10^{-2}	1.07×10^{-3}	0.428
36	0.566	0.81×10^{-2}	1.07×10^{-3}	0.424
37	0.543	0.79×10^{-2}	1.12×10^{-3}	0.448
38	0.516	0.76×10^{-2}	1.15×10^{-3}	0.475
40	0.479	0.71×10^{-2}	1.23×10^{-3}	0.512

a−d see subscript Table 2.

3.4 Natural Radiative Lifetimes in the 6snf $^3F_4$ Sequence

Calculated values for the natural radiative lifetimes (τ) of the 6snf $^3F_4$ ($13 \le n \le 40$) sequence of Ba I are collected in Table 5. In Fig. 5, the ln-ln plot of τ versus n^* is shown. It is noticed that hydrogenic model is not applicable in the region $n = 13-27$. In this region a sharp decrease in the value of the lifetime at $n = 19$ is observed. The decrease in the lifetime in the region $n = 13-19$ is due to the extended perturbation of the 6snf $^3F_4$ ($13 \le n \le 25$) Rydberg series by strong interaction with the 5d8p $^3F_4$ level [12]. The wave function of the 6s13f $^3F_4$ level contains 8.7% $|5d8p\ ^3F_4\rangle$ perturber character. The admixture of this perturber into the 6snf $^3F_4$ levels was found to grow for n increasing to 19. For the 6s18f $^3F_4$ level, the perturber character reaches 41.9%, while it becomes 42.7% in 6s19f $^3F_4$. It decreases again for $n \ge 20$, to become 26.6% for the 6s20f $^3F_4$ level and 7.4% for the 6s25f $^3F_4$ level. Moreover, Vassen et al. [21], found that, the 5d7d $^3G_5$ perturber level located at 41 607.066 cm^{-1} contains 41.4% admixture of the 6sng $^3G_5$ Rydberg series, whereas the 6s15g $^3G_5$ level located at 41 522.59 cm^{-1} contains 39.3% perturber character. The inclusion of these admixture coefficients in the calculation increases the transition probabilities for the 6snf $^3F_4$ levels with $n \le 19$ and consequently shortens their lifetime. The value of the lifetime for the 6snf $^3F_4$ levels for $n \ge 20$ is affected by the changes of the perturber character of these levels as mentioned above. On the other hand, the local perturbations of the 6snd $^3D_3$ (at $n = 27$) and 6sng $^{1,3}G_4$ (at $n = 24$) Rydberg series by the presence of the 5d7d $^3F_3$ and 5d7d $^1G_4$ perturber levels, together with the insufficient information of the 6snd $^3D_3$ Rydberg series with $n \ge 30$, Camus et al. [19], could affect the value of τ for $n \ge 34$.

In Table 6, branching ratios corresponding to transitions of 6snf $^3F_4$ levels to all lower lying even-parity 6snd $^3D_3$ and 6sng $^{1,3}G_4$, $^3G_3$, and $^3G_5$ levels are given. It should be noted that the contribution of the 6snd $^3D_3$ levels are much larger than those of the 6sng $^{1,3}G_4$, $^3G_3$ levels. The 6sng $^3G_5$ levels significantly

Table 5. Theoretical values for radiative lifetime of the 6snf $^3F_4$ sequence of Ba I.

Level	τ (μs)	Level	τ (μs)
6s13f $^3F_4$	20.2	6s26f $^3F_4$	64.7
6s14f $^3F_4$	21.4	6s27f $^3F_4$	149.1
6s15f $^3F_4$	20.1	6s28f $^3F_4$	178.7
6s16f $^3F_4$	15.8	6s29f $^3F_4$	207.6
6s17f $^3F_4$	9.6	6s30f $^3F_4$	238.6
6s18f $^3F_4$	4.4	6s31f $^3F_4$	271.4
6s19f $^3F_4$	4.7	6s32f $^3F_4$	301.8
6s20f $^3F_4$	11.9	6s33f $^3F_4$	345.4
6s21f $^3F_4$	24.4	6s35f $^3F_4$	721.5
6s22f $^3F_4$	40.7	6s36f $^3F_4$	496.4
6s23f $^3F_4$	59.6	6s38f $^3F_4$	578.5
6s24f $^3F_4$	80.4	6s40f $^3F_4$	693.5
6s25f $^3F_4$	102.7	5d8p $^3F_4$	2.7

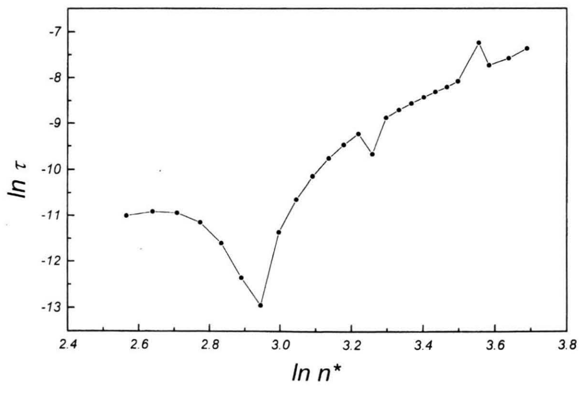

Fig. 5. ln–ln plot of the natural radiative lifetimes versus the effective principal quantum number of the odd-parity 6snf $^3F_4$ Rydberg series of Ba I (the solid line serves to guide the eye).

Table 6. Branching ratios $a(^3D_3)^a$, $a(^3G_3)^b$, $a(^{1,3}G_4)^c$, and $a(^3G_5)^d$ for the 6snf $^3F_4$ levels of Ba I.

n	$a(^3D_3)$	$a(^3G_3)$	$a(^{1,3}G_4)$	$a(^3G_5)$
13	0.806	1.12×10^{-4}	9.9×10^{-3}	0.185
14	0.806	1.20×10^{-4}	10.2×10^{-3}	0.184
15	0.839	1.20×10^{-4}	9.0×10^{-3}	0.152
16	0.880	0.91×10^{-4}	6.6×10^{-3}	0.107
17	0.940	0.52×10^{-4}	3.6×10^{-3}	0.057
18	0.981	0.19×10^{-4}	1.3×10^{-3}	0.018
19	0.994	0.016×10^{-4}	0.088×10^{-3}	0.005
20	0.969	0.041×10^{-4}	1.06×10^{-3}	0.030
21	0.928	2.00×10^{-4}	2.9×10^{-3}	0.069
22	0.880	3.10×10^{-4}	5.1×10^{-3}	0.114
23	0.834	4.10×10^{-4}	7.1×10^{-3}	0.158
24	0.792	5.00×10^{-4}	8.6×10^{-3}	0.198
25	0.756	5.60×10^{-4}	10.2×10^{-3}	0.234
26	0.868	2.70×10^{-4}	5.5×10^{-3}	0.127
27	0.680	6.60×10^{-4}	13.0×10^{-3}	0.306
28	0.668	7.10×10^{-4}	14.5×10^{-3}	0.317
29	0.644	7.50×10^{-4}	15.6×10^{-3}	0.340
30	0.623	7.80×10^{-4}	16.7×10^{-3}	0.360
31	0.604	8.00×10^{-4}	17.6×10^{-3}	0.378
32	0.573	8.10×10^{-4}	18.3×10^{-3}	0.389
33	0.567	8.50×10^{-4}	19.5×10^{-3}	0.413
35	0.971	0.055×10^{-4}	0.013×10^{-3}	0.029
36	0.518	9.50×10^{-4}	0.081×10^{-3}	0.481
38	0.489	9.30×10^{-4}	23.0×10^{-3}	0.487
40	0.462	9.50×10^{-4}	25.0×10^{-3}	0.512

[a–d] see subscript Table 2.

contribute to the decay rate of the 6snf $^3F_4$ levels, However, the contribution at $n = 35$ is much decreased in comparison with the contribution of the 6snd $^3D_3$ levels because of a perturbation of the 6snd $^3D_3$ series near $n = 27$ [19].

4. Discussion

It is well known that the lifetimes of Rydberg levels of a one-electron atom (e.g. alkali atoms) shows an $(n^*)^3$-dependence. The situation is less simple for the two-electron alkali-earth atoms, because in this case, the radiative lifetime of the Rydberg levels may be dramatically modified in the vicinity of doubly-excited perturbing states. Therefore, deviations from a simple hydrogenic model can be expected. For instance Aymar and Camus [18] measured radiative lifetimes of the even-parity 6snd $^{1,3}D_2$ $(17 \leq n \leq 35)$ levels of Ba I by selective laser excitation. Their results show a strong deviation from the hydrogenic scaling law, which was attributed to the configuration interaction of these series with 5d7d states.

In the present work calculated values of lifetime of odd-parity 6snf $^1F_3$ and $^3F_4$ levels in contrast with those of 6snf $^3F_3$ levels show deviations from the hydrogenic model as well. In this case the wave functions of 6snf $^1F_3$ $(n \geq 11)$ and $^3F_4$ $(n \geq 13)$ levels may be expanded as follows:

$$|6snf\,^1F_3\rangle = a_i|6snf\,^1F_3\rangle + b_i|6snf\,^3F_3\rangle + \sum_\alpha c_i^\alpha|5d\,8p\rangle \quad (7)$$

and

$$|6snf\,^3F_4\rangle = d_i|6snf\,^3F_4\rangle + e_i|5d\,8p\,^3F_4\rangle\,. \quad (8)$$

Here a_i, b_i and c_i^α in (7) and d_i and e_i in (8) are the MQDT mixing coefficients of the interacting channels. These wave functions have pure LS-coupling angular momenta. However, the radiative decay of a given level i depends not only on these parameters but also may be affected by perturbations of the 6snd and 6sng contributing levels.

5. Conclusion

In this report, new results for radiative lifetimes of the odd-parity 6snf $^3F_3$ $(11 \leq n \leq 40)$, $^1F_3$ $(11 \leq n \leq 40)$ and $^3F_4$ $(13 \leq n \leq 40)$ Rydberg sequences of Ba I have been calculated, using the available MQDT wave functions of these levels and all contributing even-parity levels of the 6snd and 6sng configurations, including their perturber states. The results for the nf $^1F_3$ and nf $^3F_4$ levels, in contrast with the nf $^3F_3$ levels, showed strong deviations from a hydrogenic scaling law. These deviations are attributed to the extended perturbations of many of the series involved. There is an obvious need for experimental data concerning the radiative lifetime of the Rydberg levels discussed in this work.

Acknowledgements

The Author wishes to thank Prof. W. Hogervorst for providing the experimental level energies and the MQDT parameters of the Rydberg series discussed in the text.

[1] R. Van Leeuwen, W. Ubachs, and W. Hogervorst, J. Phys. B **27,** 3891 (1994).
[2] U. Volz, D. Marger, R. Roth, and H. Schmoranzer, J. Phys. B **28,** 579 (1995).
[3] M. A. Zaki Ewiss and I. Al-Ahdali, Il-Nuovo Cim. J., D **18,** 1 (1996).
[4] A. Bizzari and M. C. E. Huber, Phys. Rev. A **42,** 5422 (1990).
[5] A. Godone and C. Novero, Phys. Rev. A **45,** 1717 (1992).
[6] J. O. Gaardsted, T. Anderson, H. K. Hangen, J. E. Hansen, and N. Vaeck, J. Phys. B **24,** 4363 (1991).
[7] J. A. Armstrong, P. Esherick, and J. J. Wynne, Phys. Rev. A **15,** 180 (1976).
[8] W. R. S. Garton and E. S. Tomkins, Astrophys. J. **158,** 1219 (1969).
[9] J. A. Armstrong, J. J. Wynne, and P. Esherick, J. Opt. Soc. Amer. **69,** 211 (1979).
[10] M. H. Abu-Taleb, Thesis, Cairo University, Egypt 1992.
[11] B. H. Post, W. Hogervorst, and W. Vassen, Phys. Rev. A **29,** 2989 (1984).
[12] B. H. Post, W. Vassen, W. Hagervorst, M. Aymar, and O. Rabaux, J. Phys. B **18,** 187 (1985).
[13] M. A. Zaki Ewiss, W. Hogervorst, W. Vassen, and B. H. Post, Z. Phys. A **322,** 211 (1985).
[14] M. A. Zaki Ewiss, W. Hogervorst, W. Vassen, and B. H. Post, Z. Phys. A **322,** 371 (1985).
[15] M. A. Zaki Ewiss, W. Hogervorst, W. Vassen, B. H. Post, and H. Wijnen, Z. Phys. A **322,** 385 (1985).
[16] M. Aymar, R. J. Champeau, C. Delsart, and J. C. Keller, J. Phys. B **14,** 4489 (1981).
[17] D. L. Bates and A. Damgaard, Phil. Trans. Roy. Soc. **242,** 101 (1949).
[18] M. Aymar and P. Camus, Phys. Rev. A **28,** 850 (1983).
[19] P. Camus, M. Dieulin, and H. I. El-Hamidy, Phys. Rev. A **26,** 379 (1982).
[20] M. Aymar, Phys. Rep. **110,** 163 (1984).
[21] W. Vassen, E. Bent, and W. Hogervorst, J. Phys. B, At. Mol. Phys. **20,** 2383 (1987).
[22] W. Vassen and W. Hogervorst, Z. Phys. **D 8,** 149 (1988).
[23] M. L. Zimmermann, M. G. Littman, M. M. Kash, and D. Kleppener, Phys. Rev. A **20,** 251 (1979).